Conserved Roles for Receptor Tyrosine Kinase Extracellular Regions in Regulating Receptor and Pathway Activity

Monica Gonzalez-Magaldi[1], Jacqueline M. McCabe[2], Haley N. Cartwright[1], Ningze Sun[1] and Daniel J. Leahy[1,2]*

[1]Dept. of Molecular Biosciences
University of Texas at Austin
100 E. 24th St. Stop A5000
Austin, TX 78712
512-471-2575

[2]Dept. of Biophysics & Biophysical Chemistry
Johns Hopkins University School of Medicine
725 N. Wolfe St.
Baltimore, MD 21205

*To whom correspondence should be addressed: dleahy@austin.utexas.edu

Summary

Receptor Tyrosine Kinases (RTKs) comprise a diverse group of cell-surface receptors that mediate key signaling events during animal development and are frequently activated in cancer. Ligand-induced dimerization is the canonical mechanism by which RTKs are thought to be activated. We show here that deletion of the extracellular regions of 10 RTKs representing 7 RTK classes or their substitution with the dimeric immunoglobulin Fc region results in constitutive receptor phosphorylation but fails to result in phosphorylation of downstream signaling effectors Erk or Akt. Conversely, substitution of RTK extracellular regions with the extracellular region of the Epidermal Growth Factor Receptor (EGFR) results in increases in Erk and/or Akt phosphorylation in response to EGF. These results indicate that the activation signal generated by the EGFR extracellular region is capable of activating at least 7 different RTK classes. Failure of phosphorylated Fc-RTK chimeras to stimulate phosphorylation of downstream effectors indicates that either dimerization and receptor phosphorylation *per se* are insufficient to activate signaling or constitutive dimerization leads to pathway inhibition.

Keywords

Receptor Tyrosine Kinase, EGFR, signaling, ERK, AKT, multimerization, dimerization

Introduction

Receptor Tyrosine Kinases (RTKs) are Type I cell-surface proteins that consist of an extracellular ligand-binding region, a membrane-spanning helix, and a tyrosine kinase-containing intracellular region (Lemmon & Schlessinger, 2010). The human genome encodes 58 RTKs that assort into 20 classes based on homologous extracellular regions and cognate ligands. Distinct RTKs classes include receptors for Epidermal Growth Factor (EGF), Insulin (Ins), Fibroblast Growth Factors (FGFs), Nerve Growth Factor (NGF), Platelet-derived Growth Factor (PDGF), and Vascular Endothelial Growth Factor (VEGF). For typical RTKs, ligand binding to the extracellular region stimulates activity of the intracellular kinase and transphosphorylation of the receptor. Receptor phosphorylation results in recruitment of downstream effectors and initiation of signaling cascades that trigger changes in cell growth, differentiation, or behavior. RTK function is essential for normal development and maintenance of multicellular organisms, and abnormal RTK activity has been associated with birth defects and many cancers (Du & Lovly, 2018; McDonell, Kernohan, Boycott, & Sawyer, 2015). RTK-targeted therapies have proven effective treatments for many RTK-associated cancers, including colon, breast, and stomach cancers (Hynes & Lane, 2005; Roskoski, 2014; Yamaoka, Kusumoto, Ando, Ohba, & Ohmori, 2018).

The canonical mechanism by which RTKs are thought to act is ligand-induced receptor dimerization (Heldin, 1995; Heldin, Lu, Evans, & Gutkind, 2016; Yarden & Schlessinger, 1987). Several observations suggest that activation of RTK signaling is more complex than simple conversion of monomers to dimers, however. Firstly, specific deletions or mutations of RTK ECRs results in constitutive receptor phosphorylation indicating an autoinhibitory role for RTK ECRs in the absence of ligand (Arevalo et al., 2001; Ekstrand et al., 1994; Merlin et al., 2009; F. H. Qiu et al., 1988; Uren, Yu, Karcaaltincaba, Pierce, & Heidaran, 1997).

Secondly, although ligand binding promotes dimerization of most RTKs and RTK extracellular regions *in vitro*, many RTKs dimerize in the absence of ligand (Clayton, Orchard, Nice, Posner, & Burgess, 2008; Del Piccolo & Hristova, 2017; Kozer et al., 2011; Liu et al., 2007; Macdonald & Pike, 2008; Martin-Fernandez, Clarke, Tobin, Jones, & Jones, 2002; Moriki, Maruyama, & Maruyama, 2001; Nagy, Claus, Jovin, & Arndt-Jovin, 2010; Saffarian, Li, Elson, & Pike, 2007; Zhang, Gureasko, Shen, Cole, & Kuriyan, 2006). Most notable in this respect are members of the Insulin Receptor (InsR) family, the subunits of which form disulfide-linked dimers and have long been thought to signal via a ligand-dependent conformational change (Lemmon & Schlessinger, 2010; Sparrow et al., 1997). Thirdly, in the case of the EGF Receptor (EGFR) artificially induced dimers result in receptor phosphorylation but not activation of downstream effectors (Liang et al., 2018; Yoshida et al., 2008), which suggests dimerization *per* se is insufficient to trigger pathway activation. Higher-order EGFR oligomers form in the presence of ligand and may be important for translating EGFR phosphorylation into pathway activation (Clayton et al., 2008; Gadella & Jovin, 1995; Huang et al., 2016; Kozer et al., 2013; Zanetti-Domingues et al., 2018).

To investigate the role of RTK extracellular regions (ECRs) in regulating RTK activity and the extent to which activation mechanisms are shared between different RTK classes, we examined the behavior of representatives of the EGFR, InsR, FGF Receptor (FGFR), VEGF Receptor (VEGFR), NGF Receptor (Trk), PDGF Receptor (PDGFR), and Met (Met and Ron) classes of RTK with deleted or substituted ECRs (Table 1). Early work had shown that EGFR/InsR chimeras retain function (Riedel, Dull, Honegger, Schlessinger, & Ullrich, 1989; Riedel, Dull, Schlessinger, & Ullrich, 1986), but such studies have not to our knowledge been extended beyond these two RTKs. We find that deletion or substitution of RTK ECRs with the dimeric immunoglobulin G Fc region generally results in constitutive phosphorylation of the receptor

but failure to increase phosphorylation of the downstream effectors Erk or Akt. Conversely, substitution of ECRs with the EGFR ECR did not always result in detectable increases in receptor phosphorylation in response to EGF but did result in EGF-dependent increases in phosphorylation of Erk and/or Akt for all RTKs assayed. These results demonstrate that RTK ECRs generate a conserved activation signal and that constitutive phosphorylation of RTKs either leads to feedback inhibition of downstream effectors or an ECR generated signal in addition to dimerization is needed to couple receptor phosphorylation to pathway activation.

Results

RTK ECRs prevent constitutive receptor phosphorylation

Deletions or mutations in several RTK extracellular regions have been associated with increased receptor phosphorylation, which has been interpreted as indicating an autoinhibitory role for these ECRs (Arevalo et al., 2001; Ekstrand et al., 1994; Merlin et al., 2009; F. H. Qiu et al., 1988; Shoelson, White, & Kahn, 1988; Uren et al., 1997). In most of these cases only a portion of the ECR is deleted, however. For example, the EGFR variant EGFRvIII, which is expressed in various cancer types, lacks roughly the N-terminal half of the ECR (aa 6-273) (Gan, Cvrljevic, & Johns, 2013). EGFRvIII is constitutively phosphorylated and able to activate downstream signaling pathways (Grandal et al., 2007; Huang et al., 2016; Schmidt, Furnari, Cavenee, & Bögler, 2003). Systematic deletion of RTK ECRs has not been carried out, however, and in isolated cases ECR deletion can lead to several-fold higher levels of receptor expression so that increased receptor phosphorylation may arise from misfolding

during biogenesis or high receptor concentrations rather than loss of autoinhibition (Kavran et al., 2014).

To provide a systematic view of the role of RTK ECRs in receptor activation and downstream signaling, C-terminally HA-tagged variants of EGFR, InsR, IGF-1R, PDGFR, VEGFR, FGFR1, FGFR2, TrkA, Met and Ron with the entire ECR deleted (Figure 1) were transiently expressed in CHO cells and lysates from these cells analyzed 24 hours after transfection by Western blot. Although phosphorylation of PDGFRα was relatively low, all ΔECR variants proved constitutively phosphorylated, consistent with an autoinhibitory function for the ECRs (Figure 2A and 2B).

To determine whether ΔECR variants are trafficked to the cell surface and rule out that the observed phosphorylation arises from aggregation in intracellular compartments, cells expressing each ΔECR variant were swollen, permeabilized, and stained with antibodies against the HA-tag and phosphotyrosine. In each case, including PDGFRα, phosphorylated forms of ΔECR variants were observed at the cell surface indicating that misfolding or aggregation during biogenesis cannot wholly account for phosphorylation of ΔECR variants (Figure 2C). Colocalization of the HA-tagged receptor ΔECR variants with cellular lectins in permeabilized cells as judged by immunofluorescence (Figure S1A) and a cell-surface biotinylation assay (Figure S1B) for all the ΔECR variants with an extracellular FLAG tag confirmed their plasma membrane localization.

Transiently expressed native RTKs traffic to the cell surface but have unprocessed intracellular forms.

Full-length native forms of each studied RTK bearing C-terminal HA-tags were expressed in CHO cells and stimulated with 100 and 500 ng/ml of their cognate ligand (Figure S2A). Cell

lysates were then assayed by Western blot for receptor expression and phosphorylation. In addition to receptor forms migrating in polyacrylamide gels at the expected molecular weights for glycosylated receptors, faster migrating and constitutively phosphorylated receptor forms with molecular weights consistent with unglycosylated or incompletely glycosylated receptors were observed for all receptors except Ron. Treatment of cell cultures with Tunicamycin and cell lysates with PNGaseF collapsed slower migrating bands into these faster migrating bands (Figure S2B), and surface biotinylation experiments demonstrated enrichment of slower-migrating, glycosylated receptor forms at the cell surface (Figure S2C). The faster migrating bands thus reflect intracellular accumulation of unglycosylated or incompletely glycosylated receptor forms. Based on this observation, ligand-dependent phosphorylation was only measured for slower migrating receptor forms. Contrary to expectation, addition of increasing concentrations of cognate ligands resulted in only modest increases in phosphorylation of the glycosylated receptor forms (Figure S2A), but, as shown below, resulted in increased phosphorylation of downstream effectors indicating functional receptors and ligands.

Fc-driven but not EGFR-ECR-driven RTK dimerization leads to robust receptor phosphorylation

To assess whether dimerization *per se* is sufficient for RTK activation or whether specific types of dimers are needed, chimeric receptors were created in which the ECRs of InsR, IGF-1R, PDGFRα, VEGFR, TrkA, FGFR1, FGFR2, Met, and Ron were substituted with (i) a constitutively dimeric immunoglobulin G constant region (Fc) or (ii) the EGFR extracellular and transmembrane regions (ECR-TM) (Figure 1). We have previously shown using FRET microscopy that substituting the EGFR ECR with Fc results in constitutive cell-surface dimers (Byrne, Hristova, & Leahy, 2020).

Fc-RTK chimeras with the Fc region fused to the EGFR, IGF-1R, PDGFRα, VEGFR, FGFR1, FGFR2, TrkA, Met, and Ron transmembrane and intracellular regions expressed well, reached the cell surface as judged by immunofluorescence (Figure S3), and were constitutively phosphorylated as judged by immunofluorescence and Western blot (Figure 3A). The Fc-InsR chimera expressed at lower levels and was less phosphorylated relative to other Fc chimeras. Even though each of the chimeric receptors with the EGFR ECR (ECR-TM) was expressed and reached the cell surface as judged by immunofluorescence (Figure S4), a clear increase in chimeric receptor phosphorylation in response to addition of EGF was only observed by Western blot for the InsR, IGF-1R, FGFR1, FGFR2, and TrkA chimeras (Figure 3B). Owing to ambiguity concerning statistical analysis of triplicate results we have opted to present band intensities of treated conditions normalized to the matched untreated condition (Figure 3B). The data points from each of three independent experiments were then plotted to enable direct visualization of the amplitudes and spread of observed changes.

EGFR-ECR-activated but not Fc- or ΔECR-activated RTKs result in robust phosphorylation of downstream effectors

RTK phosphorylation is frequently used as a proxy for RTK signaling (Lemmon & Schlessinger, 2010; Pawson, 2004), but it has been shown that phosphorylation of artificially dimerized EGFR does not necessarily lead to phosphorylation of downstream effectors (Liang et al., 2018; Sousa et al., 2012). To determine if phosphorylation of EGFR(ECR-TM)-RTK(ICR), Fc-RTK(TM-ICR), and ΔECR-RTK(TM-ICR) variants leads to phosphorylation of downstream effectors, Western blots for Erk, Akt, phospho-Erk, and phospho-Akt were carried out for each RTK variant and for native full-length receptors in the absence and presence of ligand (Figures 4 and 5). In all cases, addition of the cognate ligand to the native receptor led to increased phosphorylation of Erk, Akt, or both (Figure 4). VEGFR expression

was much lower than other RTKs, however, which may explain the more modest increases in Erk and Akt phosphorylation seen following treatment of VEGFR-expressing cells with VEGF (Figure 4). Owing to ambiguity concerning the significance of statistical analysis of triplicate results from Western blot experiments performed on multiple gels and best way to present results, we have opted to normalize integrated band intensities of treated conditions to those of untreated conditions and present these values relative to the treated condition for native EGFR. The data points for each experiment are plotted to enable direct visualization of the relative amplitudes and spread of observed changes (Figure 4B and Figure 5B).

Despite constitutive phosphorylation of the ΔECR RTKs (Figure 2B), no ΔECR RTK variant stimulated detectable increases in phosphorylation of Erk or Akt (Figure 4A). Similarly, no Fc-RTK chimera except Fc-EGFR stimulated detectable phosphorylation of Erk or Akt (Figure 4). Fc-EGFR was the most highly expressed Fc chimera, however, and only modest levels of phospho-Erk and phospho-Akt relative to wild-type EGFR in the presence of EGF were observed (Figure 4). In contrast, clear EGF-dependent phosphorylation of Erk, Akt, or both was observed for all EGFR-ECR chimeras except the VEGFR chimera, for which Erk phosphorylation was present but modest and no increase in Akt phosphorylation was observed (Figure 5). This observation is somewhat surprising given the undetectable to modest phosphorylation of many chimeras themselves when stimulated with EGF (Figure 3B).

The absence of phosphorylation of downstream effectors in cells expressing constitutively phosphorylated Fc-chimera and ΔECR RTK variants may stem from inhibitory feedback mechanisms induced by constitutive receptor phosphorylation. To determine whether Erk and Akt signaling was generally repressed in cells expressing these RTK variants, CHO cells were co-transfected with wild type EGFR and Fc-EGFR or ΔECD-EGFR in ratios that resulted in

similar expressions levels. In these cells both full length EGFR and downstream effectors became phosphorylated in response to EGF as judged by Western blot despite the presence of constitutively phosphorylated Fc-EGFR or ΔECR-EGFR variants (Figure S5). This observation indicates that Fc-EGFR and ΔECR-EGFR do not induce generalized inhibition of EGFR signaling.

Discussion

The canonical mechanism by which ligands are thought to activate RTKs is by formation of ligand-dependent receptor dimers (Heldin, 1995; Heldin et al., 2016; Yarden & Schlessinger, 1987). Although ligands drive dimerization of most RTKs (Lemmon & Schlessinger, 2010), several observations imply that regulation of receptor activity is more complex than simple conversion of monomers to dimers (Clayton et al., 2008; Del Piccolo & Hristova, 2017; Huang et al., 2016; Zanetti-Domingues et al., 2018). Using the well-studied EGFR as an example, preformed and presumably inactive EGFR dimers are present in the absence of ligand (Byrne et al., 2020; Freed, Alvarado, & Lemmon, 2015; Gadella & Jovin, 1995; Macdonald & Pike, 2008; Macdonald-Obermann, Adak, Landgraf, Piwnica-Worms, & Pike, 2013; Sako, Minoghchi, & Yanagida, 2000; Tao & Maruyama, 2008), higher-order EGFR oligomers appear in the presence of ligand (Gadella & Jovin, 1995; Huang et al., 2016; Kozer et al., 2013; Zanetti-Domingues et al., 2018), and dimerization-driven phosphorylation of EGFR can be insufficient to activate downstream signaling effectors (Liang et al., 2018; Yoshida et al., 2008).

To investigate regulatory roles of RTK ECRs beyond mediating ligand-dependent dimers and whether these roles are shared among diverse RTKs, we examined the behavior of variant

forms of 10 RTKs (EGFR, InsR, IGF-1R, PDGFRα, VEGFR, FGFR1, FGFR2, TrkA, Met, and Ron) representing 7 RTK classes. Deletion of the ECR of each RTK led to expression of a constitutively phosphorylated receptor at the cell surface consistent with a general autoinhibitory role for RTK ECRs. Increased expression levels of the ΔECR variants relative to native receptors cannot be ruled out as contributing to this phosphorylation, however. The failure of any ΔECR variant to stimulate phosphorylation of Erk or Akt despite their overexpression and relatively high phosphorylation levels implies that either ligand-bound RTK ECRs provide a signal in addition to dimerization that is needed to couple receptor phosphorylation to pathway activation or constitutive receptor phosphorylation induces feedback inhibition of downstream effectors. If an additional signal is present, the presence of Erk phosphorylation in cells expressing the oncogenic EGFRvIII (Pedersen et al., 2005; Pedersen, Tkach, Pedersen, Berezin, & Poulsen, 2004), which lacks the first two of four EGFR extracellular domains, may provide a clue to its nature. Mutations in a region in Domain IV of the EGFR ECR, which is present in EGFRvIII but not in ΔECR EGFR, have been shown to decrease EGFR activity as well as formation of higher-order EGFR oligomers (Huang et al., 2016) and this region of Domain IV may confer an activity needed to activate downstream effectors.

Although all Fc-RTK chimeras were highly expressed relative to native receptors, trafficked to the cell surface, and constitutively phosphorylated, none but Fc-EGFR led to detectable increases in phosphorylation of Erk or Akt in conditions where much lower levels of native receptors led to increased phosphorylation of Erk and/or Akt in the presence of ligand. Fc-EGFR was the most overexpressed Fc-RTK chimera but only resulted in weak phosphorylation of Erk and Akt relative to ligand-stimulated EGFR, consistent with an impaired ability of Fc-EGFR to trigger Erk or Akt activation. This result may indicate that while Fc-mediated

dimerization is sufficient to result in constitutive receptor phosphorylation it is not sufficient to trigger phosphorylation of downstream effectors. Induction of pathway inhibition by constitutive phosphorylation cannot be ruled out as underlying the absence of Erk and Akt phosphorylation, but the ability of native EGFR to activate downstream effectors in response to ligand when co-transfected with Fc-EGFR indicates that any induced pathway inhibition is not global. This observation coupled with remarkable earlier observations that artificially induced EGFR dimerization also led to receptor phosphorylation but not activation of downstream effectors raises the possibility that ligand-bound EGFR ECRs provide a signal in addition to dimerization that is essential to trigger pathway activation (Liang et al., 2018; Yoshida et al., 2008).

Conversely, although addition of EGF to EGFR (ECR-TM)-RTK chimeras did not lead to detectable increases in phosphorylation for several chimeras, increased phosphorylation of Erk and/or Akt was observed following addition of EGF to each of the EGFR(ECR-TM)-RTK(ICR) chimeras. The ability of the EGFR ECR to supply this role for at least 6 additional classes of RTKs indicates that a common signaling mechanism is shared among most if not all signaling-competent RTK ECRs. Given that dimerization *per se* may not be sufficient to trigger RTK pathway activation, it is tempting to speculate what additional shared signal may be required to trigger pathway activation. As higher-order EGFR oligomers are known to form in the presence of ligand, an intriguing possibility is that such oligomers might constitute part of this additional signal. In addition to any autoinhibitory mechanism supplied by ECRs in the absence of ligand, the need for a higher-order RTK oligomer to trigger pathway activation would minimize pathway activation from random collisions in the cell membrane. Higher-order oligomers could also contribute to downstream signaling by increasing the local concentration and stability of adaptors recruited to phosphorylated RTKs as well as potentially

altering local features of the cell membrane (Ichinose, Murata, Yanagida, & Sako, 2004; Pawson, 2004).

Collectively, the results reported here confirm and generalize an autoinhibitory role for RTK ECRs, demonstrate that the signal generated by the ligand-bound EGFR ECR is sufficient to activate members of at least seven RTK families, and hints that, as observed by others for EGFR (Liang et al., 2018; Yoshida et al., 2008), a signal in addition to dimerization may be needed by most if not all RTKs to couple receptor phosphorylation to activation of downstream effectors. Future work will be needed to confirm the presence of this additional signal and, if present, define its precise nature, whether other cellular factors are involved, and its role in RTK-associated cancers and RTK-targeted anticancer therapies.

Acknowledgements.

This work was supported by NIH R01GM099321 (DJL) and CPRIT RR160023 (DJL). We thank Pat Byrne and other Leahy lab members for advice and commentary, Pat Byrne for providing the FcEGFR clone, and Kalina Hristova for providing the VEGFR, FGFR and TrkA clones.

Author Contributions

Conceptualization, M.G-M., J.M.M., and D.J.L.; Methodology, M.G-M., J.M.M., and D.J.L.; Investigation, M.G-M., J.M.M., H.N.C., and N.S.; Writing–Original Draft, D.J.L. and M.G-M.; Writing–Review & Editing, D.J.L. and M.G-M.; Funding Acquisition, D.J.L.

Declaration of Interests

The authors declare no competing interests.

Figure Legends

Figure 1. Schematic diagram of chimeric receptors. Cartoon representations and abbreviations for each of the native or variant RTKs used in this study are shown. In addition to full-length native RTKs, which are composed of extracellular, transmembrane, and intracellular regions, variants in which the extracellular region was replaced with a constitutively dimeric murine IgGFc (Fc-RTK(TM-ICR)), the extracellular region was deleted (ΔECR), or the extracellular and transmembrane regions replaced with the human EGFR extracellular and transmembrane regions (EGFR(ECR-TM)-ICR) were created. Abbreviations for specific RTKs shown in Table 1 are substituted in the above designations to denote specific RTK variants in the text. A C-terminal HA tag added to each variant to aid uniform detection and is shown in red.

Figure 2. ΔECR variant RTKs are constitutively phosphorylated and trafficked to the plasma membrane. Western blot analysis of expression (HA-tag) and phosphorylation (EGFR pY1068, InsR/IGF-1R pY11135, or pY 4G10) of transiently-transfected CHO cells expressing HA-tagged versions of **A)** full length and ΔECR forms of EGFR, InsR, and IGF-1R with and without addition of cognate ligands, **B)** ΔECR-RTK variants of EGFR, PDGFRα, VEGFR-2, FGFR-1, FGFR-2, TrkA, Met, and Ron. β-Actin was included as a loading control, and the same amount of total protein was loaded in each well. Representative Western blots from three independent experiments are shown. **C)** Confocal microscopy images of CHO cells transfected with the indicated ΔECR RTK variant showing cell surface expression and phosphorylation for each variant. Cells were swollen in hypotonic media, washed, permeabilized and stained with an anti-HA antibody as indicated in the cartoon (HAtag-555; red), an anti-phosphotyrosine antibody (pY-488; green), and DAPI (nuclei; blue). The scale bar represents

10 µm. Non-transfected cells evident with DAPI in the same field serve as negative controls for primary and secondary antibodies. See also Figure S1 and S2.

Figure 3. All Fc-driven but not all EGFR-ECR-driven RTK dimerization leads to receptor phosphorylation. Chimeric receptors with **A)** the IgGFc domain (Fc-RTK(TM-ICR) or **B)** the EGFR extracellular and transmembrane regions (EGFR(ECR-TM)-ICR) substituted for the native ECR or ECR and transmembrane region, respectively, were transiently expressed in CHO cells and cell lysates analyzed by Western blot for expression (HA-tag) and phosphorylation (pY4G10). In the case of EGFR(ECR-TM)-ICRs, 100 ng/ml of EGF was added for 5 min before lysing the cells. All Fc-RTK receptor variants were constitutively phosphorylated, but, with the exception of EGFR-InsR, EGFR-IGF-1R, FGFR1, FGFR2 and TrkA chimeras, phosphorylation of EGFR(ECR-TM)-ICR variants chimeras did not increase notably when ligand was added. The graphic representation of the increment in phosphorylation for each chimeric receptor relative to the non-ligand added condition is shown. Dots represent an independent experiment for each condition and bars represent the mean value of the three experiments. See also Figures S3 and S4.

Figure 4. RTKs(ECR)-activated but not Fc- or ΔECR-phosphorylated RTKs trigger increased phosphorylation of downstream effectors. A) Western blot analysis of RTK variant expression (HA-tag or IGF-1R β-chain), Erk 1/2 expression (Erk 1/2), phospho-Erk 1/2 (pErk1/2), Akt expression (Akt), and phospho-Akt (pAkt) levels for native RTKs with and without cognate ligand, Fc-RTK(TM-ICR) (Fc), and ΔECR (ΔECR) variants of the indicated RTKs transiently expressed in CHO cells. β-Actin was included as a loading control, and the same amount of total protein was loaded in each well. **B)** Quantification and graphic representation of the downstream activation obtained from WB analysis. Each dot represents

an independent experiment for each condition, and the bar heights represent the mean values for these experiments.

Figure 5. EGFR(ECR-TM)-RTK chimeras activate downstream pathways in response to EGF. A) Western blot analysis of cell lysates from CHO cells transiently expressing the indicated chimeric RTKs in which the EGFR ECR-TM region was substituted for the native ECR-TM with and without EGF (or cognate ligands) are shown. Chimeric receptor EGFR(ECR-TM)-RTK expression (HA-tag or IGF-1R β-chain), phospho-Erk 1/2 (pErk1/2), Erk 1/2 expression (Erk 1/2), phospho-Akt (pAkt), and Akt expression (Akt) were assessed. β-Actin was included as a loading control, and the same amount of total protein was loaded in each well. **B)** Quantification and graphic representation of phospho-Erk and phospho-Akt levels obtained from WB analysis normalized as detailed in results. Each dot represents an independent experiment, and the bar heights represent the mean values for three experiments (except for pERK for Fc-InsR and Fc-IGF-1R, which have two).

Table 1. Receptor Tyrosine Kinases Studied

Name	Abreviation	Ligand	Class
Epidermal growth factor receptor	EGFR	Human Epidermal growth factor	I
Insulin like growth factor receptor	IGF-1R	Human Insulin like growth factor	II
Insulin receptor	InsR	Recombinant Human Insulin Protein	II
Platelet-derived growth factor receptor alpha	PDGFRa	Human Platelet-Derived Growth Factor AA	III
Vascular endothelial growth factor receptor type 2	VEGFR2	Human Vascular Endothelial Growth Factor-121	IV
Fibroblast growth factor type 1 and 2	FDFR1/2	Human Basic Fibroblast Growth Factor	V
Tropomyosin receptor kinase A	TrkA	Human β-Nerve Growth Factor	VII
Hepatocyte growth factor receptor	Met	Human Hepatocyte Growth Factor	X
Macrophage-stimulating protein receptor	Ron	Recombinant Human Macrophage Stimulating Protein	X

Table 2. Amino acid sequences of RTK variant termini and junctions

Protein	Variant	N to C sequence
IgGFc	Fc	SSVFIFP… HTEKSLSHS
EGFR	Full length	MRPSGTA… PQSSEFIGA
	ΔECD	IPS**IATGM**… PQSSEFIGA
	Fc-ICD	
	ECR-TM	MRPSGTA … **ALGIGLFM**
IGF-1R	Full length	MKSGSGGG … ALPLPQSSTC
	ΔECD	**LIIALPVAV** … ALPLPQSSTC
	Fc-ICD	
InsR	Full length	MATGGRR … TLPRSNPS
	ΔECD	IAK**IIIGPLI …** TLPRSNPS
	Fc-ICD	
PDGFRα	Full length	MGTSHPAFL … SDLVEDSFL
	ΔECD	TVA**AAVLVL**…SDLVEDSFL
	Fc-ICD	
VEGFR2	Full length	GLPSVSLDL … GTTLSSPPV
	ΔECD	LE**IIILVG**… GTTLSSPPV
	Fc-ICD	
FDFR1	Full length	MWSWKCLL … LANGGLKRR
	ΔECD	LE**IIIYCT**… LANGGLKRR
	Fc-ICD	
FDFR2	Full length	MVSWGRFIC … PHINGSVKT
	ΔECD	YLE**IAIYCI**… PHINGSVKT
	Fc-ICD	
TrkA	Full length	MLRGGRRGQ … PPVYLDVLG
	ΔECD	VAVG**LAVF**… PPVYLDVLG
	Fc-ICD	
Met	Full length	MKAPAVLAP…TRPASFWETS
	ΔECD	NFT**GLIAGV**… RPASFWETS
	Fc-ICD	
Ron	Full length	MELLPPLPQS … RPLSEPPRPT
	ΔECD	QST**LLGIPS** … PQSSEFIGA
	Fc-ICD	

Transmembrane regions are indicated in bold letters

The Fc-ICR variants have the Fc sequence followed by ΔECD sequence

Materials and Methods

Key Resources Table

Key Resources Table				
Reagent type (species) or resource	**Designation**	**Source or reference**	**Identifiers**	**Additional information**
gene	Full length human IGF-1R		NM_000875.4	
gene	Full length human InsR		NM_000208.2	
gene	Full length human EGFR		NM_005228.3	
gene	Full length human PDGFRa		NM_006206	
gene	Full length human VEFR2		NM_002253.2	
gene	Full length human FGFR1		NM_023110.2	
gene	Full length human FGFR2		NM_000141.4	

gene	Full length human TrkA		NM_001012331.1	
gene	Full length human Ron		NM_002447.2	
gene	Full length human Met		NM_000245.2	
gene	IgG Fc mouse		U65534	
cell line	Chinese hamster ovary cells CHO-K1	ATCC	Cat# CCL-61 (RRID: CVCL_0214)	
antibody	Mouse anti-Phosphotyrosine clone 4G10	EMD Millipore	Cat # 05-321 (RRID: AB_568857)	WB(1:100) IF(1:200)
antibody	Rabbit anti-HA Polyclonal antibody	Thermo Fisher Scientific	Cat # PA1-985 (RRID: AB_1958085)	WB(1:100) IF(1:200)
antibody	Rabbi anti phospho-EGFR pTyr1068 antibody	Thermo Fisher Scientific	Cat # 44-788G (RRID: AB_2533754)	Dilution 1:1000
antibody	Rabbit anti-EGFR D1D4J	Cell Signaling Technology	Cat # 54359 (RRID: AB_2799458)	Dilution 1:200
antibody	Rabbit anti IGF-1R β-chain D23H3	Cell Signaling Technology	Cat # 9750 (RRID: AB_2797674)	Dilution 1:1000
antibody	Rabbit anti Erk1/2 MAPK p42/p44	Cell Signaling Technology	Cat # 4695 (RRID: AB_390779)	Dilution 1:1000
antibody	Rabbit anti pErk P-p42/p44 MAPK	Cell Signaling Technology	Cat # 9101 (RRID: AB_331646)	Dilution 1:1000

	(Erk1/2) Thr202/Tyr 204			
antibody	Rabbit anti-AKT1	Sigma-Aldrich	Cat # SAB4300575 (RRID: AB_10624863)	Dilution 1:1000
antibody	Rabbit anti-β-Actin	Cell Signaling Technology	Cat # 4968 (RRID: AB_2313904)	Dilution 1:2000
antibody	Secondary Goat anti-rabbit-680RD	Li-Cor	Cat # 926-68071	Dilution 1:15000
antibody	Secondary Goat anti-mouse IgG_{2b}-800CW	Li-Cor	Cat # 926-32352	Dilution 1:15000
antibody	Rabbit anti-Phospho-Akt (Ser473)	Cell Signaling Technology	Cat # 4060 (RRID: AB_2315049)	Dilution 1:1000
antibody	Rabbit anti-Hsp90α	Cell Signaling Technology	Cat # 4877 (RRID: AB_2233307)	Dilution 1:1000
antibody	DYKDDDDK Tag Polyclonal Antibody	Thermo Fisher Scientific	Cat # PA1-984B (RRID: AB_347227)	Dilution 1:2000
antibody	Goat anti rabbit IgG Alexa fluor 555	Thermo Fisher Scientific	Cat # A-21428 (RRID: AB_2535849)	Dilution 1:500
antibody	Donkey anti mouse IgG Alexa fluor 555	Invitrogen	Cat # A-31570 (RRID: AB_2536180)	Dilution 1:500
antibody	Rabbit anti phospho-IGF-I receptor β Tyr1135/36/ IR β	Cell Signaling Technology	Cat # 2969 (RRID: AB_11178660)	Dilution 1:1000

	Tyr1150/1151			
recombinant DNA reagent	vector pαH	Aricescu et al. 2006	N/A	
recombinant DNA reagent	pcDNA 3.1	Invitrogen	Cat # V79020	
peptide, recombinant protein	Human Epidermal growth factor EGF	(C. Qiu et al., 2009)	N/A	
peptide, recombinant protein	Human Insulin like growth factor IGF-1	(Kavran et al., 2014)	N/A	
peptide, recombinant protein	Recombinant Human Insulin Protein	Novus Biologicals	Cat # NBP1-99193	
peptide, recombinant protein	Human Platelet-Derived Growth Factor AA	Cell Signaling	Cat # 8913	
peptide, recombinant protein	Human Basic Fibroblast Growth Factor	Cell Signaling	Cat # 8910	
peptide, recombinant protein	Human Vascular Endothelial Growth Factor-121	Cell Signaling	Cat # 8908	
peptide, recombinant protein	Human β-Nerve Growth Factor	Cell Signaling	Cat # 5221	

peptide, recombinant protein	Human Hepatocyte Growth Factor	Sigma-Aldrich	Cat # H9661	
peptide, recombinant protein	Recombinant Human Macrophage Stimulating Protein	RεD systems	Cat # 352-MS-010	
commercial assay or kit	Pierce™ Cell Surface Biotinyla-tion and Isolation Kit	Pierce	Cat # A44390	
commercial assay or kit	Pierce™ BCA Protein Assay	Thermo Fisher Scientific	Cat # 23225	
chemical compound, drug	Wheat Germ Agglutinin Alexa Fluor 488 conjugate	Invitrogen	Cat # W11261	
chemical compound, drug	DAPI (4',6-Diamidino-2-Phenylindole, Dihydrochloride)	Thermo Fisher Scientific	Cat # 62247	
chemical compound, drug	ProLong™ Diamond antifade mountant	Thermo Fisher Scientific	Cat # P36965	
software, algorithm	Fiji	Fiji contributors	https://imagej.net/Fiji/Downloads	
software, algorithm	Prism Graphpad	GraphPad	https://www.graphpad.com/scientific-software/prism/	

software, algorithm	Zen lite software	Zeiss	https://www.zeiss.com/microscopy/us/products/microscope-software/zen-lite.html	
software, algorithm	Image studio™ lite software	Li-Cor	https://www.licor.com/bio/image-studio-lite/download	

Cell culture, Transfection and Expression

CHO-K1 cells were maintained in adherent culture in DMEM: F12 (Gibco) supplemented with 5% Fetal Bovine Serum (Gibco). For transient transfections, CHO-K1 cells were plated in six-well plates at 0.5×10^6 cells/well and transfected with 1 µg of each indicated expression plasmid using Lipofectamine 2000 (Thermo Fisher Scientific) according to the manufacturer's protocol. After 18 hours cells were washed three times with 2 ml Ham's F12 supplemented with 1 mg/ml BSA and serum starved in this medium for 3 hr at 37°C. Each specific ligand was added in designated wells, 100 ng/ml EGF for 5 min, 150 ng/ml IGF1, 200 nM (1.14 µg/ml) insulin for 30 min, 100 ng/ml PDGF-AA, 100 ng/ml FGF-basic, 100 ng/ml hVEGF-121, 100 ng/ml Human β-Nerve Growth Factor, 100 ng/ml Hepatocyte Growth Factor, 100 ng/ml Macrophage Stimulating Protein and incubated 15 min at 37°C. Wells were washed with ice-cold phosphate buffered saline and lysed for 30 min at 4°C in 250 µl of RIPA buffer (50 mM Tris pH 8.0, 150 mM NaCl, 1% (v/v) NP40, 0.5% (w/v) sodium deoxycholate, 0.1% (w/v) sodium dodecyl sulfate) supplemented with 1 mM activated Na_3VO_4, Pierce protease inhibitor minitablet (Thermo Fisher Scientific), Benzonase nuclease (Sigma), and 10 nM iodoacetamide to prevent disulphide-bond formation during lysis. The total protein concentration of clarified lysates was determined using the BCA assay (Smith et al., 1985), and all lysates were adjusted to lowest total protein concentration using RIPA buffer.

473 Cotransfection experiments were performed in the same growth conditions, with the ratio of
474 DNAs encoding different variants adjusted to obtain similar levels of expression for both
475 variants. For the pair EGFR:ΔECR-EGFR the DNA ratio was 1:1 with 1.5 µg of each
476 expression plasmid transfected using 1mg/ml PEI as transfecting agent as described (Longo,
477 Kavran, Kim, & Leahy, 2013) (*3:1 ratio of PEI to DNA (w/w)*). For the EGFR:Fc-EGFR pair
478 the ratio was 2:0.5. Cells were lysed 20 h post transfection following serum starvation
479 described above.
480
481 *Expression vector design*
482 DNA sequences encoding each RTK variant were cloned into modified versions of the
483 expression vector pαH, which was derived from pHLSec by insertion of an alternative multiple
484 cloning site (Aricescu, 2006). Modifications to pαH included: removal of the signal sequence
485 encoding region, addition of a region encoding a C-terminal HA tag, and addition of coding
486 sequences for the EGFR (ECR-TM) that facilitated cloning of chimeric receptors.
487 DNA sequences encoding full length human IGF-1R, InsR, EGFR VEGFR2, PDGFRα,
488 FGFR1 and FGFR2, TrkA, Ron, and Met cDNAs were used to generate full length and
489 chimeric receptors. Deletions of the ECR for each receptor were generated by PCR. Fc-RTK
490 chimeric receptors substituted regions encoding the mouse IgG Fc region for native ECRs prior
491 to the TM-ICR RTK of interest (Table 2). Transmembrane boundaries for each RTK were
492 guided by domain annotation of mRNA and protein sequences from NCBI.
493
494 *Western Blots*
495 Cell lysates with normalized total protein concentrations were mixed with SDS sample buffer
496 and boiled, separated by SDS-PAGE (Novex 4-12% Tris-Glycine Mini Protein Gels, 1.0mm,
497 15 well (Life Technologies, EC6025)), and transferred using the iBlot® Dry Blotting System

with iBlot® Transfer Stacks to a nitrocellulose membrane (Life Technologies, IB301001). The membrane was blocked with 3% low fat milk in TBS, and proteins were labeled by incubation with the selected primary antibody and the corresponding Infrared dye secondary antibody, which was detected using a Li-Cor Odyssey Clx Near IR imaging system. The amount loaded in each well was normalized by BCA assay. β-actin was used as loading control as a qualitative confirmation of overall protein abundance present in each experiment. Band intensities were integrated using Image Studio Lyte software. Independent experiments for each condition are presented as dots in the graphic representations with bar heights representing the mean value of multiple measurements. Statistical analyses are not reported owing to ambiguity interpreting the meaning of statistics for triplicate experiments. We present instead the plots showing data points from each experiment and their mean.

Immunofluorescence and confocal microscopy

CHO-K1 cells grown on glass cover slips were transfected with 1 μg of the indicated DNA. At 24 hours post transfection, cells were fixed in 4% paraformaldehyde for 15 min at room temperature, blocked and permeabilized with PBTG buffer (0.1% Triton X-100, 1% bovine serum albumin (BSA), and 1 M glycine in PBS) or non-permeabilizing buffer (PBTG without Triton X-100) for 15 min. Samples were incubated with the selected primary antibody diluted in 1% BSA in PBS for 1 h at room temperature, washed with PBS and incubated with the corresponding secondary antibody for 30 min. Wheat germ agglutinin coupled with Alexa fluor 488 was added together with the secondary antibody. DAPI was used for DNA staining. Samples were then mounted in Prolong Gold anti fade reagent (Invitrogen) and cells observed with a Zeiss 710 Laser Scanning Confocal (ZeissCF) microscope.

To swell cells after transfection, cells were incubated in hypotonic media (10% DMEM in H2O, 25 mM HEPES, 50 mM EDTA and 1mM Sodium orthovanadate) for 30 min at 37°C

523 and washed with PBS supplemented with 1 mM Sodium orthovanadate. Cells were then fixed,
524 permeabilized, and incubated with primary and secondary antibodies as described above.
525
526 *Cell surface protein biotinylation for SDS-PAGE analysis*
527 Four 100 mm plates of CHO cells were transfected with 15 µg DNA of expression plasmids
528 directing expression of each full-length RTK full and cell-surface biotinylation and isolation
529 of cell surface proteins carried out according to the manufacturer's instructions (Pierce, Cat #
530 A44390). For biotinylation of the ΔECR variants, an extracellular FLAG tag was added to the
531 N-terminus of each variant.
532
533 *Deglycosylation assay*
534 CHO cells were transfected with 1 µg of the indicated expression plasmid, and 8 h post-
535 transfection cells were treated with 2µg/ml Tunicamycin for 20 h. Cells were then treated with
536 2U/ml PNGase F for 2h at 37 °C, washed, and lysed as previously described.
537
538 **Supplemental Figure Legends**
539
540 **Supplemental Figure 1. ΔECR forms of all RTKs are trafficked to the cell surface. A)**
541 Confocal microscopy images of CHO cells transiently transfected with the indicated ΔECR
542 RTK variant showing cell surface expression of each variant. Cells were swollen in hypotonic
543 media, washed, permeabilized and stained with an anti-HA antibody (HAtag-555; red) and
544 wheat germ agglutinin to label the cell surface (WGA-488; green). **B)** N-terminal FLAG-
545 tagged ΔECR variants of the indicated RTKs were transiently expressed in CHO cells. Cell
546 surface proteins were biotinylated, separated by using a streptavidin-affinity matrix, and
547 expressed proteins detected by anti-FLAG Western blot (left). Anti-HSP90 Western blot of

streptavidin-affinity Elution and Flow Through fractions showing that cytoplasmic proteins were not detectably biotinylated.

Supplemental Figure 2. Cell-surface expression, glycosylation and ligand-dependent phosphorylation of native RTKs. A) HA-tagged forms of the indicated RTKs were transiently expressed in CHO cells, and expression and phosphorylation levels in the presence and absence of ligand determined by Western blot using anti-HA (HA-tag) and anti-phosphotyrosine (pY4G10) antibodies. Stars indicate slower migrating bands that represent fully processed receptors. Quantification and graphic representation of the band intensities are shown. The phosphorylation intensity was normalized to the expression and the increment was made relative to each receptor without ligand. Dots represent individual values from independent experiments for each sample and the bars represent the calculated mean value of the three experiments. β-Actin was included as a loading control. **B)** Anti-HA Western blot of lysates from CHO cells transiently expressing the indicated RTKs without deglycosylation treatment (-) or treated with Tunicamycin for 20 hours followed by treatment of cell lysates with PNGase F (DG). **C)** Anti-HA Western blot of indicated proteins transiently expressed in CHO cells following biotinylation of cell surface proteins and separation using a streptavidin-affinity matrix.

Supplemental Figure 3. Fc-RTK(TM-ICR) forms of all RTKs are trafficked to the cell surface. Confocal microscopy images of untransfected CHO cells and CHO cells transiently transfected with the indicated Fc-RTK(TM-ICR) variants showing cell surface expression of each variant. Cells were swollen in hypotonic media, washed, permeabilized and stained with an anti-Fc antibody (Anti Fc mouse; red), wheat germ agglutinin to label the cell surface (WGA-488; green), and DAPI (nuclei; blue). The scale bar represents 20 μm.

Supplemental Figure 4. EGFR(ECR-TM)-ICR forms of all RTKs are trafficked to the cell surface. Confocal microscopy images of untransfected CHO cells and CHO cells transiently transfected with the indicated EGFR(ECR-TM)-ICR RTK variant showing cell surface expression of each variant. Cells were swollen in hypotonic media, washed, permeabilized and stained with an anti-EGFR ECR antibody (EGFR ECR; red), wheat germ agglutinin to label the cell surface (WGA; green), and DAPI (nuclei; blue). The scale bar represents 10 μm.

Supplemental Figure 5. EGFR is able to activate downstream effectors in response to ligand in cells expressing constitutively-phosphorylated Fc-EGFR or ΔECR-EGFR. CHO cells were co-transfected with native EGFR plus Fc-EGFR(TM-ICR) or ΔECR-EGFR, 100 ng/ml EGF were added and lysates were analyzed by Western blot using an anti-HA tag (HAtag), EGFR phospho tyrosine 1068 (pY1068), phospho-Erk 1/2 (pErk1/2), Erk 1/2 expression (Erk 1/2), phospho-Akt (pAkt), and Akt expression (Akt).

References

Arevalo, J. C., Conde, B., Hempstead, B. I., Chao, M. V., Martín-Zanca, D., & Pérez, P. (2001). A novel mutation within the extracellular domain of TrkA causes constitutive receptor activation. *Oncogene, 20*(10), 1229-1234.

Byrne, P. O., Hristova, K., & Leahy, D. J. (2020). Ligand-independent EGFR oligomers do not rely on the active state asymmetric kinase dimer. *bioRxiv*, 2020.2004.2024.056077.

Clayton, A. H., Orchard, S. G., Nice, E. C., Posner, R. G., & Burgess, A. W. (2008). Predominance of activated EGFR higher-order oligomers on the cell surface. *Growth Factors, 26*(6), 316-324.

Del Piccolo, N., & Hristova, K. (2017). Quantifying the Interaction between EGFR Dimers and Grb2 in Live Cells. *Biophys J, 113*(6), 1353-1364.

Du, Z., & Lovly, C. M. (2018). Mechanisms of receptor tyrosine kinase activation in cancer. *Mol Cancer, 17*(1), 58.

Ekstrand, A. J., Longo, N., Hamid, M. L., Olson, J. J., Liu, L., Collins, V. P., et al. (1994). Functional characterization of an EGF receptor with a truncated extracellular domain expressed in glioblastomas with EGFR gene amplification. *Oncogene, 9*(8), 2313-2320.

Freed, D. M., Alvarado, D., & Lemmon, M. A. (2015). Ligand regulation of a constitutively dimeric EGF receptor. *Nat Commun, 6*, 7380.

Gadella, T. W., & Jovin, T. M. (1995). Oligomerization of epidermal growth factor receptors on A431 cells studied by time-resolved fluorescence imaging microscopy. A stereochemical model for tyrosine kinase receptor activation. *J Cell Biol, 129*(6), 1543-1558.

Gan, H. K., Cvrljevic, A. N., & Johns, T. G. (2013). The epidermal growth factor receptor variant III (EGFRvIII): where wild things are altered. *FEBS J, 280*(21), 5350-5370.

Grandal, M. V., Zandi, R., Pedersen, M. W., Willumsen, B. M., van Deurs, B., & Poulsen, H. S. (2007). EGFRvIII escapes down-regulation due to impaired internalization and sorting to lysosomes. *Carcinogenesis, 28*(7), 1408-1417.

Heldin, C. H. (1995). Dimerization of cell surface receptors in signal transduction. *Cell, 80*(2), 213-223.

Heldin, C. H., Lu, B., Evans, R., & Gutkind, J. S. (2016). Signals and Receptors. *Cold Spring Harb Perspect Biol, 8*(4), a005900.

Huang, Y., Bharill, S., Karandur, D., Peterson, S. M., Marita, M., Shi, X., et al. (2016). Molecular basis for multimerization in the activation of the epidermal growth factor receptor. *Elife, 5*.

Hynes, N. E., & Lane, H. A. (2005). ERBB receptors and cancer: the complexity of targeted inhibitors. *Nat Rev Cancer, 5*(5), 341-354.

Ichinose, J., Murata, M., Yanagida, T., & Sako, Y. (2004). EGF signalling amplification induced by dynamic clustering of EGFR. *Biochem Biophys Res Commun, 324*(3), 1143-1149.

Kavran, J. M., McCabe, J. M., Byrne, P. O., Connacher, M. K., Wang, Z., Ramek, A., et al. (2014). How IGF-1 activates its receptor. *Elife, 3*.

Kozer, N., Barua, D., Orchard, S., Nice, E. C., Burgess, A. W., Hlavacek, W. S., et al. (2013). Exploring higher-order EGFR oligomerisation and phosphorylation--a combined experimental and theoretical approach. *Mol Biosyst, 9*(7), 1849-1863.

Kozer, N., Henderson, C., Jackson, J. T., Nice, E. C., Burgess, A. W., & Clayton, A. H. (2011). Evidence for extended YFP-EGFR dimers in the absence of ligand on the surface of living cells. *Phys Biol, 8*(6), 066002.

Lemmon, M. A., & Schlessinger, J. (2010). Cell signaling by receptor tyrosine kinases. *Cell, 141*(7), 1117-1134.

Liang, S. I., van Lengerich, B., Eichel, K., Cha, M., Patterson, D. M., Yoon, T. Y., et al. (2018). Phosphorylated EGFR Dimers Are Not Sufficient to Activate Ras. *Cell Rep, 22*(10), 2593-2600.

Liu, P., Sudhaharan, T., Koh, R. M., Hwang, L. C., Ahmed, S., Maruyama, I. N., et al. (2007). Investigation of the dimerization of proteins from the epidermal growth factor receptor family by single wavelength fluorescence cross-correlation spectroscopy. *Biophys J, 93*(2), 684-698.

Longo, P. A., Kavran, J. M., Kim, M. S., & Leahy, D. J. (2013). Transient mammalian cell transfection with polyethylenimine (PEI). *Methods Enzymol, 529*, 227-240.

Macdonald, J. L., & Pike, L. J. (2008). Heterogeneity in EGF-binding affinities arises from negative cooperativity in an aggregating system. *Proc Natl Acad Sci U S A, 105*(1), 112-117.

Macdonald-Obermann, J. L., Adak, S., Landgraf, R., Piwnica-Worms, D., & Pike, L. J. (2013). Dynamic analysis of the epidermal growth factor (EGF) receptor-ErbB2-ErbB3 protein network by luciferase fragment complementation imaging. *J Biol Chem, 288*(42), 30773-30784.

Martin-Fernandez, M., Clarke, D. T., Tobin, M. J., Jones, S. V., & Jones, G. R. (2002). Preformed oligomeric epidermal growth factor receptors undergo an ectodomain structure change during signaling. *Biophys J, 82*(5), 2415-2427.

McDonell, L. M., Kernohan, K. D., Boycott, K. M., & Sawyer, S. L. (2015). Receptor tyrosine kinase mutations in developmental syndromes and cancer: two sides of the same coin. *Hum Mol Genet, 24*(R1), R60-66.

Merlin, S., Pietronave, S., Locarno, D., Valente, G., Follenzi, A., & Prat, M. (2009). Deletion of the ectodomain unleashes the transforming, invasive, and tumorigenic potential of the MET oncogene. *Cancer Sci, 100*(4), 633-638.

Moriki, T., Maruyama, H., & Maruyama, I. N. (2001). Activation of preformed EGF receptor dimers by ligand-induced rotation of the transmembrane domain. *J Mol Biol, 311*(5), 1011-1026.

Nagy, P., Claus, J., Jovin, T. M., & Arndt-Jovin, D. J. (2010). Distribution of resting and ligand-bound ErbB1 and ErbB2 receptor tyrosine kinases in living cells using number and brightness analysis. *Proc Natl Acad Sci U S A, 107*(38), 16524-16529.

Pawson, T. (2004). Specificity in signal transduction: from phosphotyrosine-SH2 domain interactions to complex cellular systems. *Cell, 116*(2), 191-203.

Pedersen, M. W., Pedersen, N., Damstrup, L., Villingshøj, M., Sønder, S. U., Rieneck, K., et al. (2005). Analysis of the epidermal growth factor receptor specific transcriptome: effect of receptor expression level and an activating mutation. *J Cell Biochem, 96*(2), 412-427.

Pedersen, M. W., Tkach, V., Pedersen, N., Berezin, V., & Poulsen, H. S. (2004). Expression of a naturally occurring constitutively active variant of the epidermal growth factor receptor in mouse fibroblasts increases motility. *Int J Cancer, 108*(5), 643-653.

Qiu, C., Tarrant, M. K., Boronina, T., Longo, P. A., Kavran, J. M., Cole, R. N., et al. (2009). In vitro enzymatic characterization of near full length EGFR in activated and inhibited states. *Biochemistry, 48*(28), 6624-6632.

Qiu, F. H., Ray, P., Brown, K., Barker, P. E., Jhanwar, S., Ruddle, F. H., et al. (1988). Primary structure of c-kit: relationship with the CSF-1/PDGF receptor kinase family--oncogenic activation of v-kit involves deletion of extracellular domain and C terminus. *EMBO J, 7*(4), 1003-1011.

Riedel, H., Dull, T. J., Honegger, A. M., Schlessinger, J., & Ullrich, A. (1989). Cytoplasmic domains determine signal specificity, cellular routing characteristics and influence ligand binding of epidermal growth factor and insulin receptors. *EMBO J, 8*(10), 2943-2954.

Riedel, H., Dull, T. J., Schlessinger, J., & Ullrich, A. (1986). A chimaeric receptor allows insulin to stimulate tyrosine kinase activity of epidermal growth factor receptor. *Nature, 324*(6092), 68-70.

Roskoski, R. (2014). The ErbB/HER family of protein-tyrosine kinases and cancer. *Pharmacol Res, 79*, 34-74.

Saffarian, S., Li, Y., Elson, E. L., & Pike, L. J. (2007). Oligomerization of the EGF receptor investigated by live cell fluorescence intensity distribution analysis. *Biophys J, 93*(3), 1021-1031.

Sako, Y., Minoghchi, S., & Yanagida, T. (2000). Single-molecule imaging of EGFR signalling on the surface of living cells. *Nat Cell Biol, 2*(3), 168-172.

Schmidt, M. H. H., Furnari, F. B., Cavenee, W. K., & Bögler, O. (2003). Epidermal growth factor receptor signaling intensity determines intracellular protein interactions, ubiquitination, and internalization. *Proc Natl Acad Sci U S A, 100*(11), 6505-6510.

Shoelson, S. E., White, M. F., & Kahn, C. R. (1988). Tryptic activation of the insulin receptor. Proteolytic truncation of the alpha-subunit releases the beta-subunit from inhibitory control. *J Biol Chem, 263*(10), 4852-4860.

Smith, P. K., Krohn, R. I., Hermanson, G. T., Mallia, A. K., Gartner, F. H., Provenzano, M. D., et al. (1985). Measurement of protein using bicinchoninic acid. *Anal Biochem, 150*(1), 76-85.

Sousa, L. P., Lax, I., Shen, H., Ferguson, S. M., De Camilli, P., & Schlessinger, J. (2012). Suppression of EGFR endocytosis by dynamin depletion reveals that EGFR signaling occurs primarily at the plasma membrane. *Proc Natl Acad Sci U S A, 109*(12), 4419-4424.

Sparrow, L. G., McKern, N. M., Gorman, J. J., Strike, P. M., Robinson, C. P., Bentley, J. D., et al. (1997). The disulfide bonds in the C-terminal domains of the human insulin receptor ectodomain. *J Biol Chem, 272*(47), 29460-29467.

Tao, R. H., & Maruyama, I. N. (2008). All EGF(ErbB) receptors have preformed homo- and heterodimeric structures in living cells. *J Cell Sci, 121*(Pt 19), 3207-3217.

Uren, A., Yu, J. C., Karcaaltincaba, M., Pierce, J. H., & Heidaran, M. A. (1997). Oncogenic activation of the alphaPDGFR defines a domain that negatively regulates receptor dimerization. *Oncogene, 14*(2), 157-162.

Yamaoka, T., Kusumoto, S., Ando, K., Ohba, M., & Ohmori, T. (2018). Receptor Tyrosine Kinase-Targeted Cancer Therapy. *Int J Mol Sci, 19*(11).

Yarden, Y., & Schlessinger, J. (1987). Self-phosphorylation of epidermal growth factor receptor: evidence for a model of intermolecular allosteric activation. *Biochemistry, 26*(5), 1434-1442.

Yoshida, T., Okamoto, I., Okabe, T., Iwasa, T., Satoh, T., Nishio, K., et al. (2008). Matuzumab and cetuximab activate the epidermal growth factor receptor but fail to trigger downstream signaling by Akt or Erk. *Int J Cancer, 122*(7), 1530-1538.

Zanetti-Domingues, L. C., Korovesis, D., Needham, S. R., Tynan, C. J., Sagawa, S., Roberts, S. K., et al. (2018). The architecture of EGFR's basal complexes reveals autoinhibition mechanisms in dimers and oligomers. *Nat Commun, 9*(1), 4325.

Zhang, X., Gureasko, J., Shen, K., Cole, P. A., & Kuriyan, J. (2006). An allosteric mechanism for activation of the kinase domain of epidermal growth factor receptor. *Cell, 125*(6), 1137-1149.

Figure 1

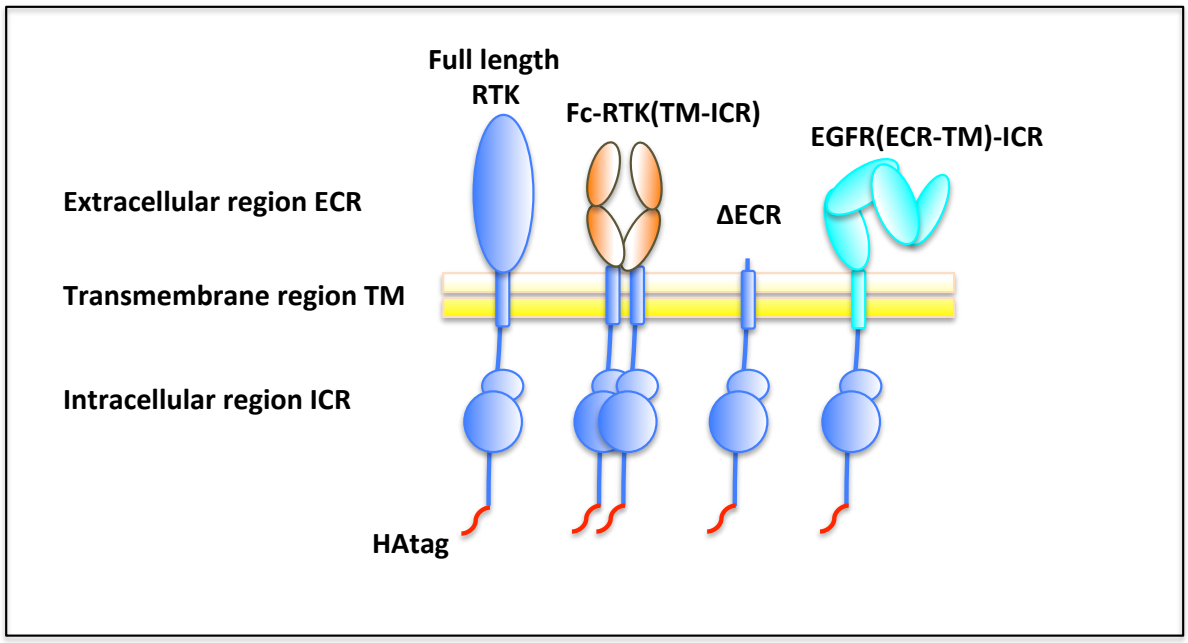

743 **Figure 2**

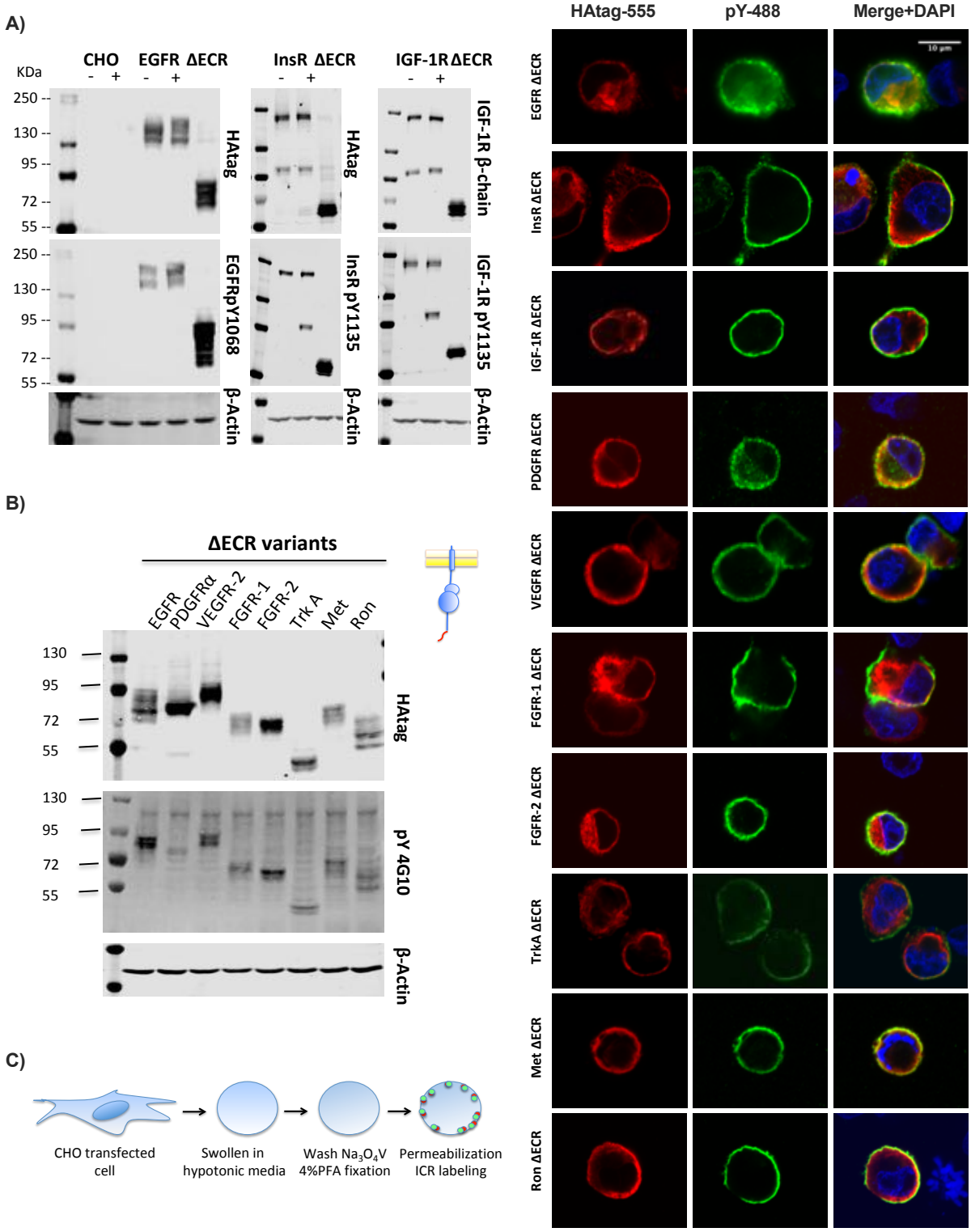

744
745

Figure 3

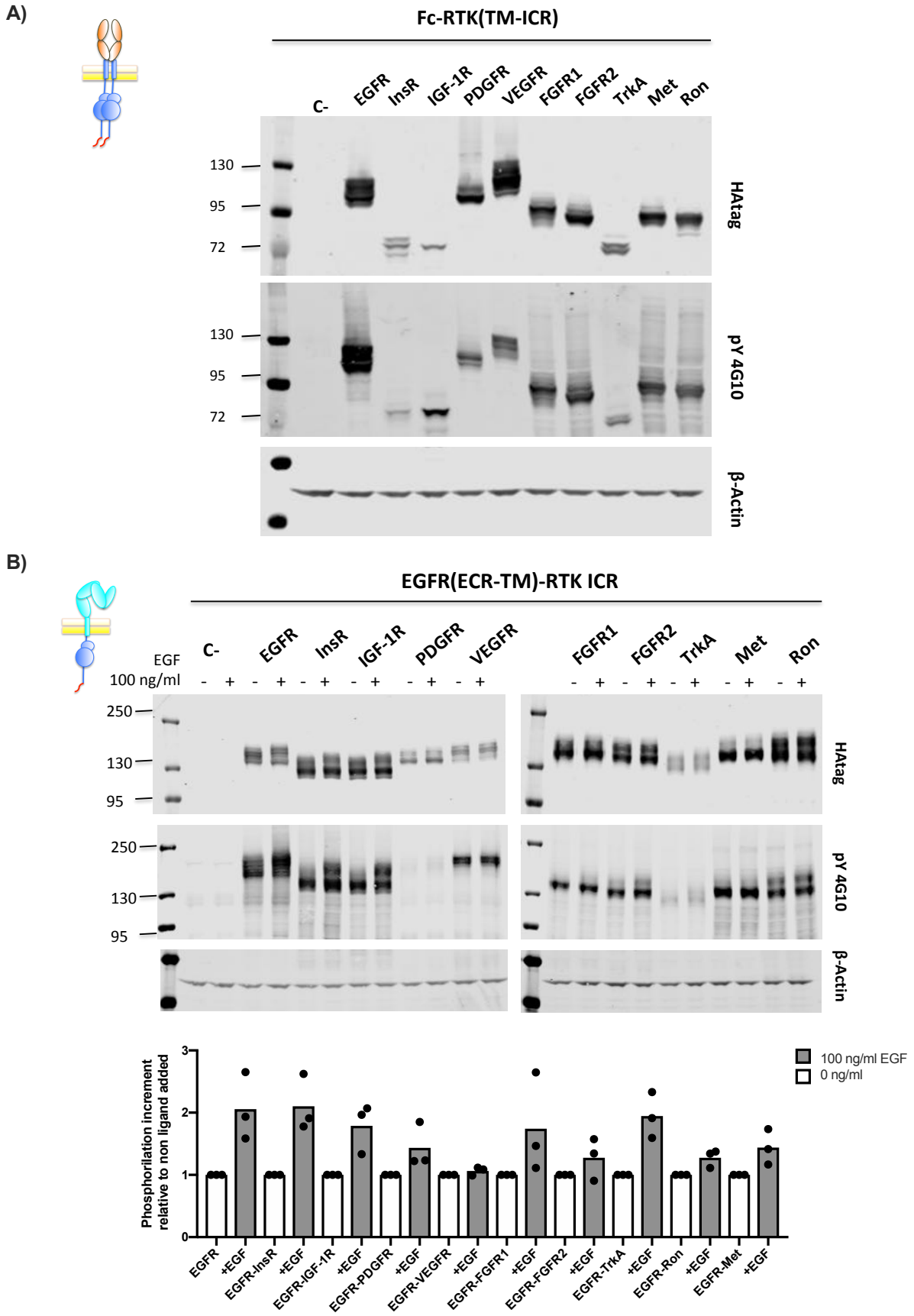

Figure 4

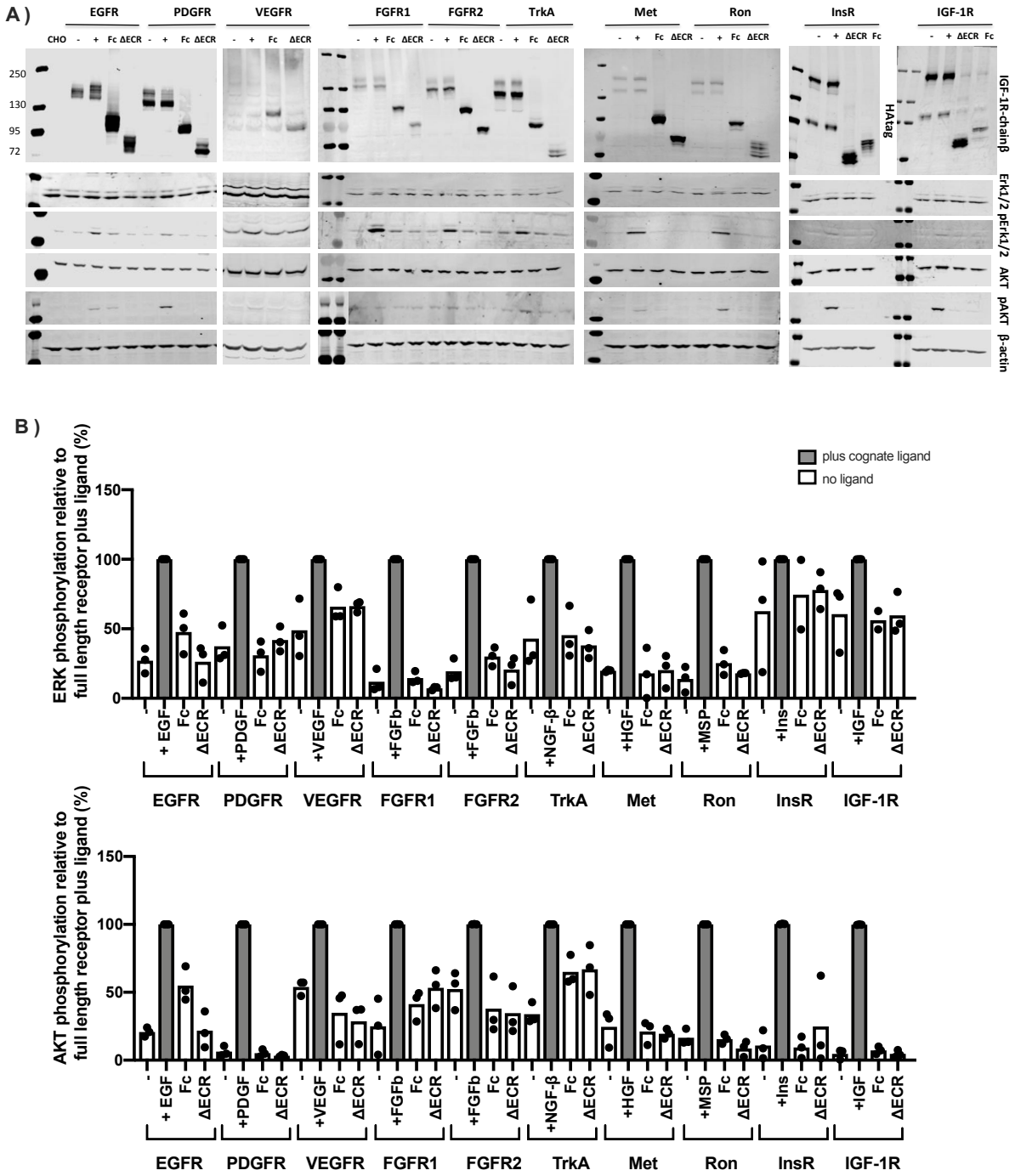

752 **Figure 5**

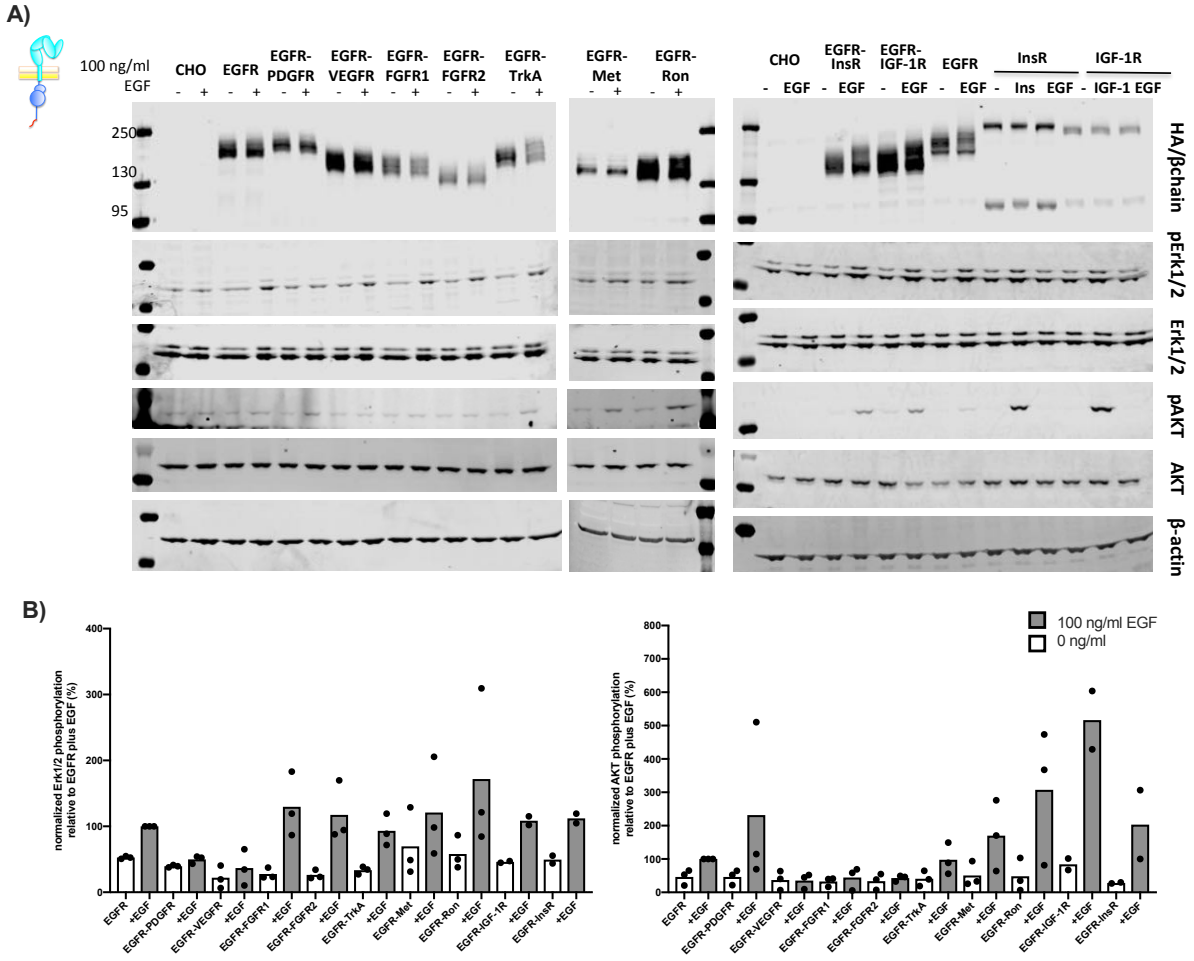

753
754

755 **Supplementary Figure 1**

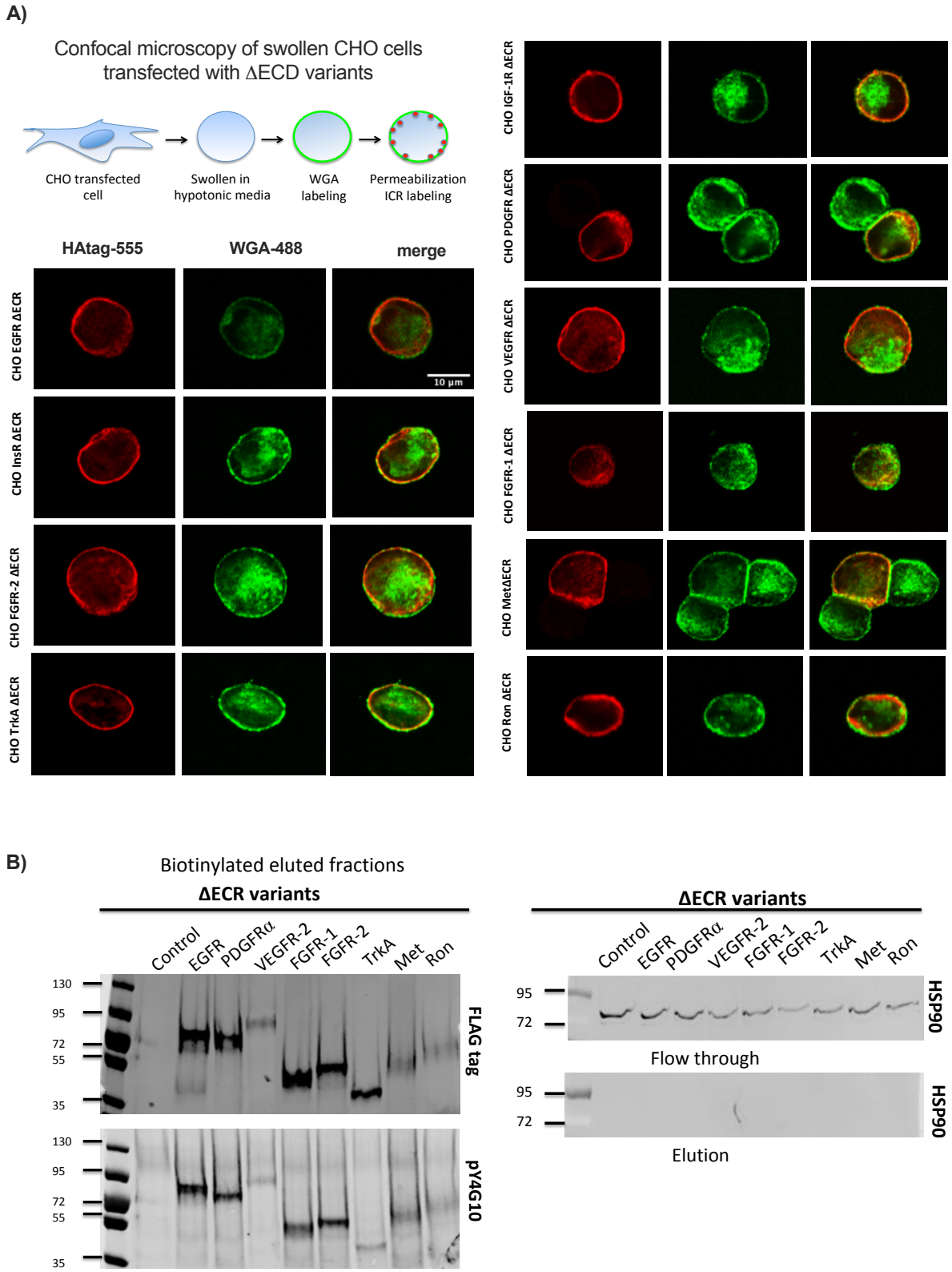

756
757

Supplementary Figure 2

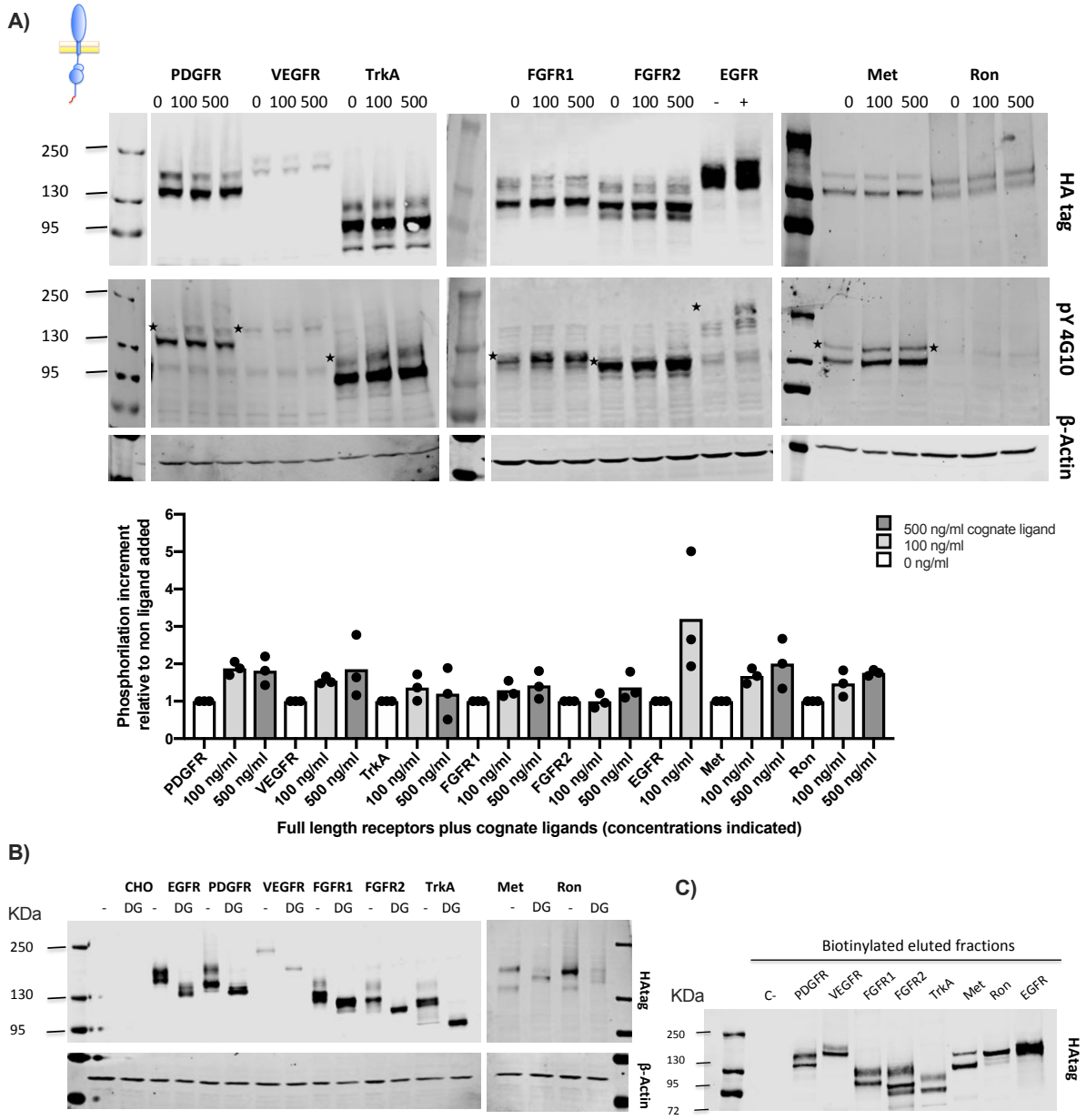

761 **Supplementary Figure 3**

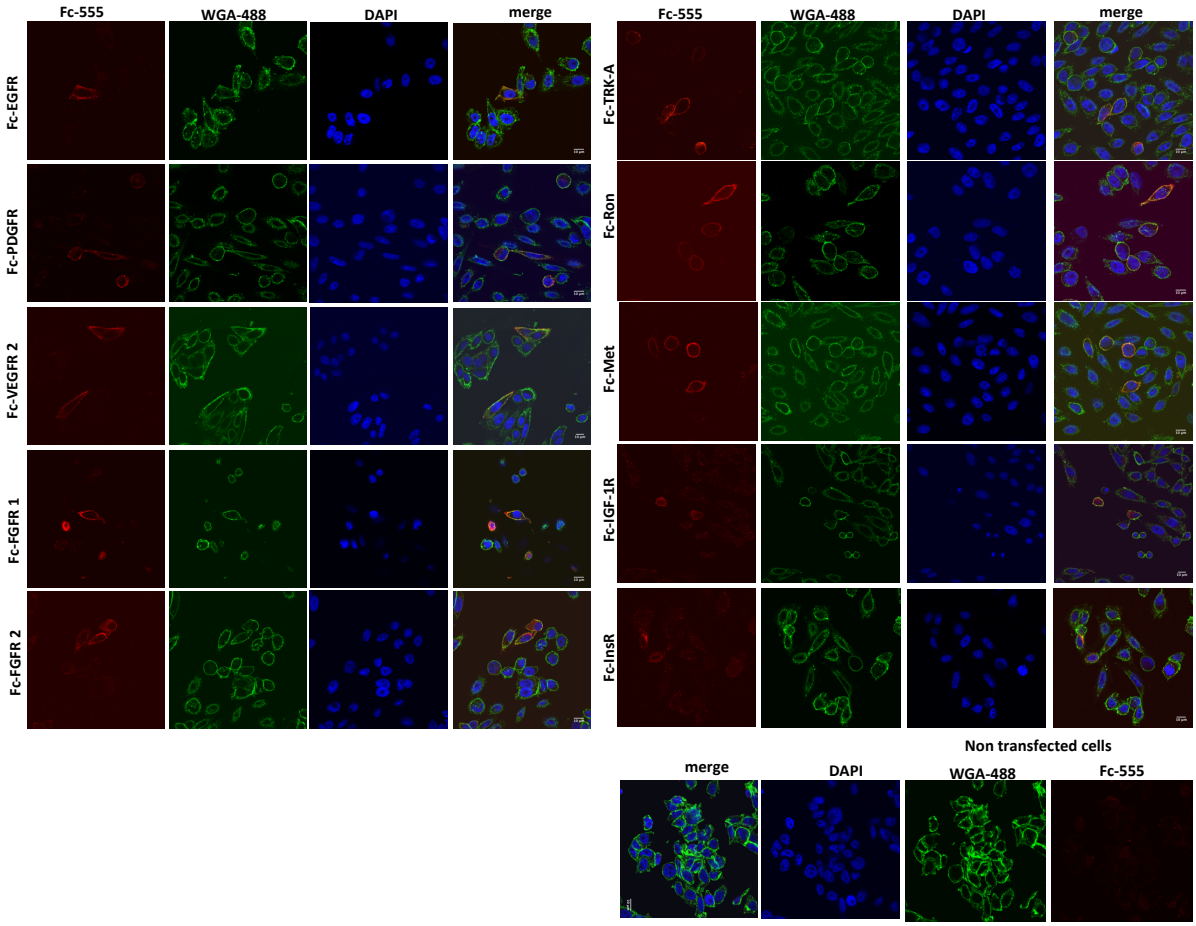

762
763

764 **Supplementary Figure 4**

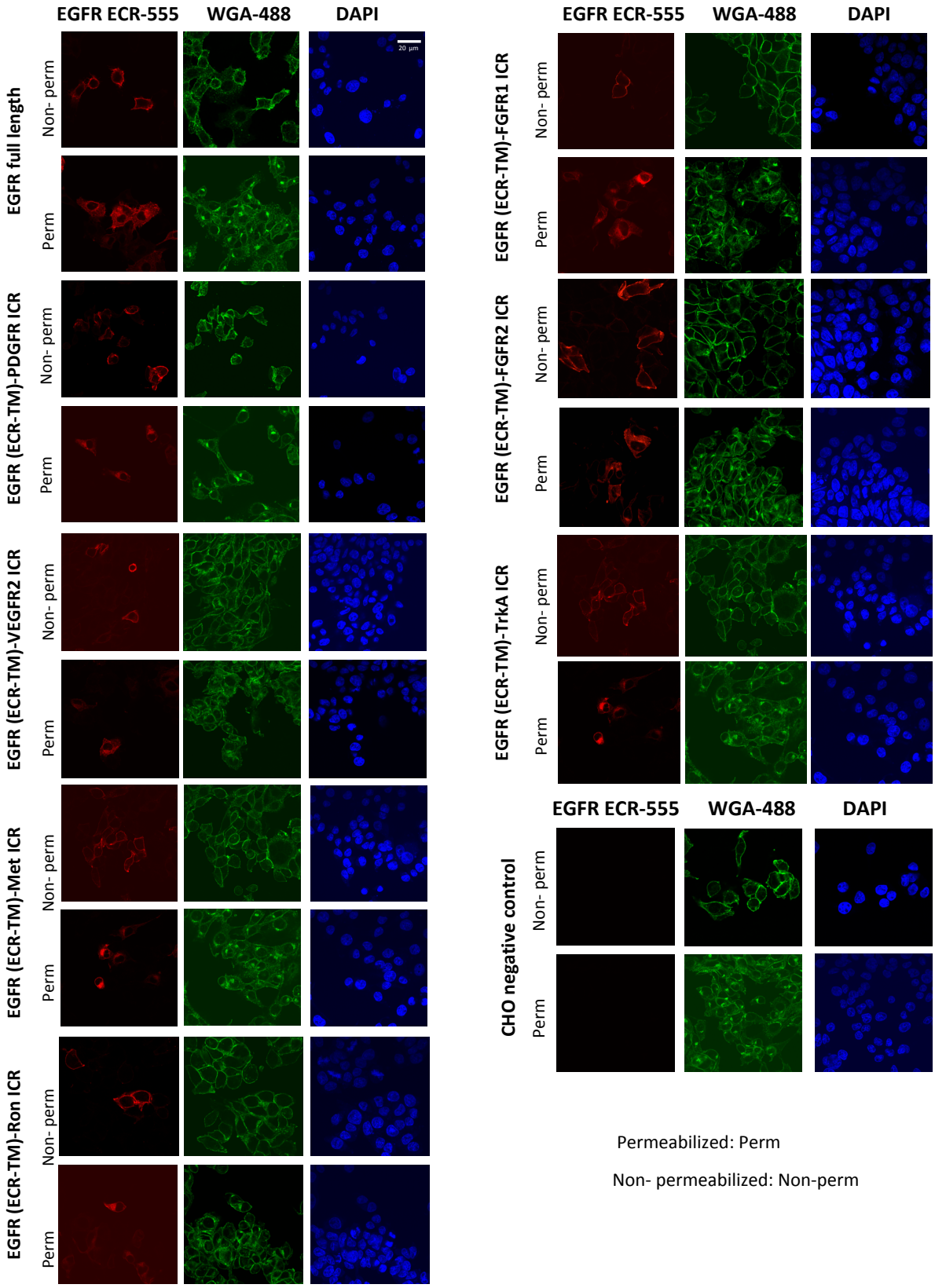

765
766

Supplementary Figure 5